Journal of Elasticity **65:** 1–31, 2001.

Interaction of Fractures in Tensile Bars with Non-Local Spatial Dependence

CAMILLO DE-LELLIS[1] and GIANNI ROYER-CARFAGNI[2]
[1]*Scuola Normale Superiore, Piazza dei Cavalieri, I56100 Pisa, Italy*
[2]*Dipartimento di Ingegneria Civile, Università di Parma, Parco Area delle Scienze 181/A, I43100 Parma, Italy. E-mail: royer@aem.umn.edu*

Received 22 August 2000; in revised form 19 November 2001

Abstract. We propose to determine the displacement field $u\colon \mathcal{I} \subset \mathbb{R} \to \mathbb{R}$ of a 1-D bar extended in a hard device by minimizing a non-local energy functional of the type

$$\Pi[u] := \int_{\mathcal{I}} U\left(u'(x) + \frac{1}{K} \sum_{x_i \in J_u} [u](x_i)\ \rho(x - x_i)\right) \mathrm{d}x + \sum_{x_i \in J_u} \varphi([u](x_i)),$$

where K is a material parameter, $[u](x_i)$ denotes the jump of u at x_i and $J_u \subset \mathcal{I}$ the set of all jump points. For appropriate choices of the bulk energy $U(\cdot)$, of the surface energy $\varphi(\cdot)$ and of the weight function $\rho(\cdot)$, we prove an existence theorem for minimizers in the space $SBV(\mathcal{I})$ of special bounded variation functions and we qualitatively discuss their form by investigating the corresponding Euler–Lagrange equations. We show that for sufficiently large values of the bar elongation, minimizers of the energy are discontinuous and, most of all, the non-local term $[u](x_i)\rho(x - x_i)$ influences the relative position among the jump points, a finding that is of crucial importance to reproduce the experimental evidence.

Mathematics Subject Classifications (2000): 74A45, 74A50, 74R20.

Key words: nonlinear elasticity, variational model, fracture mechanics, non-local model, damage.

1. Introduction and Setting

The gross response of a great variety of different types of materials, ranging from quasi-brittle solids to ductile metals, is governed by an underlying microscopic transition indicated by the localization of exceptionally large strains in layers of evanescent thickness, which can be modelled as surfaces of discontinuity for the deformation field. In general, two limit cases can be distinguished. In cleavage fractures, characteristic of a brittle response, it is the component of the displacement vector normal to such surface that suffers discontinuity, whereas in shear fractures (or slip layers), indicative of plastic deformation, discontinuity exists only in the tangential component. The response of bars whose lateral dimensions are small with respect to their length is usually described by one-dimensional theories in which the occurrence of fracturing, whether it be of the cleavage or shear type, is modelled by the discontinuity in the displacement field.

Although fractures are as a rule irreversible, consistent 1-D models have been conceived of through a variational approach, which has the great advantage of naturally providing equilibrium relations and boundary conditions. With reference to an axis x coinciding with the axis of the bar, the interval $\mathcal{I} \subset \mathbb{R}$ is made to represent the natural undistorted state of the body, and the scalar function $u\colon \mathcal{I} \to \mathbb{R}$, the average axial displacement for particles of the cross section initially at x. Following the original idea by Dugdale [11] and Barenblatt [3], substantial progress has recently been achieved by equating the bar equilibrium configurations with the stationary and minimum points of strain energies of the form

$$\int_{\mathcal{I}} U\big(u'_a(x)\big)\,\mathrm{d}x + \sum_{x_i \in J_u} \varphi\big([u](x_i)\big). \tag{1.1}$$

Here u'_a denotes the absolutely continuous part of the generalized derivative Du (in the sense of distribution) of the displacement field u, $[u](x_i)$ represents the jump of $u(x)$ at $x = x_i$, while $J_u \subset \mathcal{I}$ is the set of all jump points of u. The function $U(\cdot)$, referred to as the "*bulk*" strain energy density, interprets the elasticity of the material between two consecutive discontinuities, whereas $\varphi(\cdot)$, the "*fracture*" or "*interfacial*" energy, models the energy expended in overcoming the intermolecular forces at the jump surfaces. By considering a simple quadratic expression for $U(\cdot)$ and varying only the shape of $\varphi(\cdot)$, a broad spectrum of different response types, ranging from brittle to plastic, has been obtained by Del Piero [8, 9]. His study suggests that the essence of the difference in the material's mechanical properties depends mainly on the type of resistance that the crack surfaces offer to their separation. This dichotomy between "bulk" and "fracture" response is evident in functionals of the type (1.1), where the two contributions are clearly separated.

Nevertheless, experimental observations have provided a wealth of evidence that the effects of strain localization are not confined to the discontinuity surfaces alone. In general, localized deformations affect the material response throughout a whole neighborhood, so that fractures might interact decisively with each other. Such an effect has been discussed in [14, 15] for elastic-plastic metal bars. In this case, it was observed that yielding of one layer produces a condition equivalent to a stress concentration at the boundary of the yielded portion, which influences the behavior of the neighboring parts and produces a chain reaction. At the mesoscopic level, as represented in Figure 1, this causes the orderly formation of slip bands,

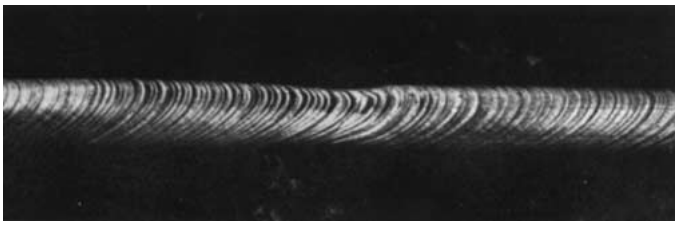

Figure 1. Stretched copper–aluminun crystal (from an experiment by Elam [12]).

which at the macroscopic level are responsible for the well-known oscillations in the stress-strain diagram usually referred to as the Portevin–Le Chatelier effect [15]. The case of quasi-brittle materials is governed by other causes, though similar "non-local" effects are in play, since the opening of a macro-crack is accompanied by the appearance of a cloud of micro-cracks in its neighborhood, usually referred to as the *process zone*, which may strongly affect the material properties of nearby portions (experimental evidence is reported in [6]).

Attempts to describe the interactions between fractures through models of the type (1.1), for example, by trying to incorporate into $\varphi(\cdot)$ the energy expended to deform the bar portions surrounding a crack, may lead to incomplete results. In fact, the location of the discontinuity surfaces remains undetermined in model (1.1), since it is clear that the energy level does not change if the jump points are moved along the bar, provided the size of the jump remains the same. On the other hand, we believe that the surprising regularity with which localized-strain layers develop deserves closer examination, as it may prove to be decisive in understanding the material behavior.

Here, we propose to determine the displacement field $u\colon \mathcal{I} \subset \mathbb{R} \to \mathbb{R}$ of a 1-D bar stretched in a hard device by minimizing a non-local energy functional of the type

$$\int_{\mathcal{I}} U\left(u'_a(x) + \frac{1}{K}\sum_{x_i \in J_u} [u](x_i)\rho(x - x_i)\right) \mathrm{d}x + \sum_{x_i \in J_u} \varphi\big([u](x_i)\big), \tag{1.2}$$

where K is a material parameter and ρ is a weight function. The underlying idea for this model consists in accounting for any possible non-local effects of fracturing by introducing the term $[u](x_i)\rho(x - x_i)$ into the argument for the bulk energy $U(\cdot)$. By properly defining constant K, the integral of ρ can be set equal to one, so that ρ and K represent the *shape* and *strength* of the non-local contribution: values of K approaching 1 are representative of strong interactions, whereas for $K \to \infty$ the functional (1.2) reduces to (1.1).

The aim of this paper is to furnish a *mathematical description* of the minimization problem for functional (1.2). But, before doing this, in Section 2 we present a simple problem in linear elasticity, which should provide, albeit tentatively, a motivation for having considered energies of the type (1.2), allowing at the same time a physical interpretation of the weight function $\rho(\cdot)$. Successively, after having stated the problem in more precise mathematical terms in Section 3, in Section 4 we shall prove an existence theorem for a wide range of choices of the bulk and surface energies $U(\cdot)$ and $\varphi(\cdot)$. Due to the presence of possible discontinuities, the natural space in which we settle the variational problem is the space $SBV(\mathcal{I})$ of functions of special bounded variation, refined by physical restrictions (i.e., conditions $u'_a \geqslant -1$ and $[u] \geqslant 0$, assuring the injectivity of deformations) on the class of admissible functions, that come into play in our existence proof. In Section 5 we set forth the necessary conditions for minimizers by considering the first variation of (1.2) and the corresponding Euler–Lagrange equations. The possible shape of minimizers for

bars stretched in a hard device are finally discussed in Section 6, where it is shown how the presence of the non-local term restricts the position of possible fractures along the bar.

2. Set-up and Motivation

There is perhaps a common characteristic in the response of tensile bars made of different materials such as metals, ceramics, polymers or geomaterials. After a first, pseudo-linear elastic period, they all show a more or less abrupt deviation from linearity, which careful experiments reveal to be the consequence of strain localization in layers of evanescent thickness. In other words, deformation occurs locally and does not take place uniformly throughout the length of the bar: when one element or layer yields, it strains several per cent almost instantly and then nearly stops, while the yielding is transferred to other portions.

The simplest way to represent in full the strain-localization process is probably the cohesive-crack model introduced in the early sixties by Barenblatt [3] and Dugdale [11]. A cohesive crack is nothing else than a fictitious crack able to transfer stress from one face to the other. In different materials there are different physical sources for cohesive cracks and it is remarkable that essentially the same model holds for many distinct micro-mechanisms [17]. In crystalline solids the source is at the nano-scale: cohesive forces recall the atomic attraction forces and fracture energy represents the work expended to push atoms beyond the sphere of interatomic activity. In conglomerates such as ceramics, rocks or concrete, the explanation is mesoscopic, i.e. grain bridging or aggregate frictional interlock; in clay or wood cohesive forces may arise from crack overlapping and in fibrous composites from fiber bridging [4]. But also metals, whose plastic properties are due to slip concentrated in thin (Lüder) bands, can be set in this category. Slip layers, in substance, are equivalent to cohesive cracks, since the relative translation of the atomic lattice produces a discontinuity in the displacement field without definite rupture. This is why, in the following, the term “crack” should be understood in a sense much broader than “material separation”.

Another noteworthy feature, as already mentioned in the Introduction, is that cracks nucleate in a precise order, at surprisingly regular intervals. This is a clear sign of a reciprocal interference. In classical linear elastic 2-D or 3-D fracture mechanics, this is captured by the elastic interaction produced by distinct fractures, but the effect degenerates in the one-dimensional case, at least for models of the type (1.1). This section is in the direction of trying to motivate, with a simple example, why introducing in the bulk energy a non-local term of the displacement jump only, as in (1.2), should provide a comprehensive view of the crack-interaction phenomenon. The model that follows is necessarily explanatory rather than exhaustive at this time, but it is expected that at least some of the questions mentioned will be clarified by further studies.

Consider a three-dimensional tensile bar with length L and constant cross section. A Cartesian system (x, y, z) is assumed with x directed according to the bar axis so that, if $\Omega \subset \mathbb{R}^2$ and $\mathcal{I} \subset \mathbb{R}$ denote the undistorted cross section and the interval $[0, L]$, respectively, the bar natural undistorted reference configuration is $\mathcal{B} \equiv \mathcal{I} \times \Omega = \{(x, y, z)\colon\ x \in \mathcal{I}, (y, z) \in \Omega\}$. The displacement field leading to the deformed configuration will be represented by $\mathbf{u}$ of components u_1, u_2 and u_3 in the x, y and z direction, whereas $\varepsilon_{ij} = \frac{1}{2}(u_{i,j} + u_{j,i})$ and σ_{ij}, $i, j = 1, 2, 3$, will denote the strain and stress components.

The shape of an equilibrium crack is certainly very complicated, but from a purely descriptive point of view, we may consider the same model originally proposed by Hillerborg [16] for quasi-brittle materials, where a rough crack is idealized as a flat crack, at right angle to the specimen axis. In mathematical terms, the occurrence of a Hillerborg crack is detected by a jump in the axial component of the displacement field. Thus, denoting with $[u_1](\cdot, y, z)$ the jump of $u_1(\cdot, y, z)$, the fracture opening at point (y, z) of the cracked cross section $x = \xi$ is represented by $[u_1](\xi, y, z)$.

For convenience, we think of decomposing the actual strain ε_{ij} in the cracked bar in the form

$$\varepsilon_{ij} = \varepsilon^0_{ij} + \varepsilon^s_{ij}, \tag{2.1}$$

where ε^0_{ij} represents the state of strain if no cracks were present, whereas ε^s_{ij} is the perturbation due to the presence of cracks. In particular, if the bulk material is homogeneous isotropic and linear-elastic, the state of stress of an uncracked bar is uniaxial and defined by the only axial component $\sigma_{11} \equiv \sigma_0$. The corresponding strain thus reads

$$\varepsilon^0_{ij} = \left(\frac{1+\nu}{E}\delta_{i1}\delta_{j1} - \frac{\nu}{E}\delta_{ij}\right)\sigma_0, \tag{2.2}$$

where δ_{ik} denotes the Kronecker's symbol and E and ν are the Young's modulus and Poisson's ratio, respectively.

In the classical linear-elastic-fracture-mechanics (LEFM) framework, the second term ε^s_{ij} may be easily evaluated. In fact, due to the linear character of the equations, ε^s_{ij} coincides with the strain field when the crack faces are opened by a pressure σ_0. Thus, referring to the undistorted configuration as customary in LEFM, ε^s_{ij} can be calculated through a surface integral extended to the crack plane once the appropriate Green function is known.⋆ The case of a cohesive crack may appear slightly different, since a definite material separation is absent. Nevertheless, experimental tests on plastic as well as quasi-brittle materials have clearly evidenced that *strain localization produces distortions* in a neighborhood of the process layer, which result in a condition equivalent to a stress concentration at the boundary of the neighboring portions. Such a distortion may be due to an abrupt change of the

⋆ This procedure, classical in LEFM, is explained in detail, for example, in Chapter 8.4 of [5].

cross section, to elastic material portions embedded in plastically bent *lamellae*, or to the breaking up of the internal crystalline structure. In metals, the effect of the stress-concentration at the boundary of a slip plane is considered responsible for the gap between the upper and lower yield point, for the progressive and equidistant appearance of slip bands, and for the stress oscillations at yielding [7]. Similar effects on quasi-brittle materials have been discussed at length in the recent book by Bažant and Planas [4].

It is plausible to assume that the amount of distortion at the borders of a cohesive crack is proportional to crack opening. Since the surrounding portions remain, presumably, elastic, we may calculate the strain field $\varepsilon_{ij}^{s,\xi}(x, y, z)$ at (x, y, z) due to the formation of one crack at $x = \xi$ through an expression of the type,

$$\varepsilon_{ij}^{s,\xi}(x, y, z) = \int_{\Omega} \widetilde{G}_{ij}\big[(x, y, z), (\xi, \eta, \zeta)\big][u_1](\xi, \eta, \zeta)\, \mathrm{d}\eta\, \mathrm{d}\zeta. \tag{2.3}$$

Here $\widetilde{G}_{ij}[(x, y, z), (\xi, \eta, \zeta)]$ is the appropriate Green's function, representing the strain components at (x, y, z) when a unitary distortion is nucleated at (ξ, η, ζ). At this stage, we are not interested in finding the exact form of $\widetilde{G}_{ij}$ but, nevertheless, interesting properties can be deduced from arguments of a very general nature.

First of all, by De-Saint Venant's principle, we know that $\widetilde{G}_{ij}[(\cdot, \cdot, \cdot), (\xi, \eta, \zeta)]$ practically vanishes at a distance from (ξ, η, ζ) of the same order of the bar diameter.

Furthermore, suppose that cracks nucleate at a distance of several diameters far from the bar ends.* For what the determination of $\widetilde{G}_{ij}[(x, y, z), (\xi, \eta, \zeta)]$ is concerned, it is not a significant error to consider the two half-bars $x < \xi$ and $x > \xi$ to be semi-infinite. Thus, the plane $x = \xi$ can be considered a plane of geometrical as well as of mechanical symmetry. It follows that the Green's function may be written in the form

$$\widetilde{G}_{ij}\big[(x, y, z), (\xi, \eta, \zeta)\big] = G_{ij}\big[(y, z), (\eta, \zeta), x - \xi\big]. \tag{2.4}$$

Finally, we may suppose that $G_{ij}[(y, z), (\eta, \zeta), x - \xi]$ is not influenced by the presence of other cracks, even when they lie in a neighborhood of $x = \xi$. This assumption may be justified in the case of elastic plastic materials, whose plastic deformation is due to lattice slipping. We can reasonably expect that the elastic properties of a homogeneous crystalline lattice are not affected when the slipping amount equals a multiple of the interatomic distance. In fact, despite some atoms are substituted by others, the atomic spacing remains unaffected. Thus, the effect of a distortion at $x = \xi$ can go undisturbed through a slip plane. A similar conclusion holds, more or less accurately according to the specific case, for quasi-brittle materials. In fact, since cohesive cracks induce no definite material separation [4], it

* At this point, we are not dealing with the very difficult issue of the border effects, i.e. when cracks form close to the bar ends. The periodic boundary conditions (6.2) considered later on, will allow to bypass this crucial problem.

is not unrealistic to assume that elastic strains can "flow" also through the cracked surface.

Assume now that cracks open maintaining fixed the fracture-surface profile. If this is represented by $f(\eta, \zeta)$, we can write

$$[u_1](\xi, \eta, \zeta) = f(\eta, \zeta)[\overline{u}_1](\xi), \tag{2.5}$$

where $[\overline{u}_1](\xi)$ denotes the average jump in the x direction, i.e.

$$[\overline{u}_1](\xi) = \frac{1}{A}\int_\Omega [u_1](\xi, \eta, \zeta)\,\mathrm{d}\eta\,\mathrm{d}\zeta, \tag{2.6}$$

being A the cross-sectional area.

Expression (2.3), taking into account (2.4), thus becomes

$$\varepsilon_{ij}^{s,\xi}(x, y, z) = [\overline{u}_1](\xi)\int_\Omega G_{ij}\big[(y, z), (\eta, \zeta), x - \xi\big] f(\eta, \zeta)\,\mathrm{d}\eta\,\mathrm{d}\zeta. \tag{2.7}$$

But if the Green's function is not altered by the presence of neighboring discontinuities, the effect of multiple cracks, provided the strain remains small and the local rotation moderate, can be considered by superimposing the strain field they generate. Thus, we can write in (2.1)

$$\varepsilon_{ij}^{s}(x, y, z) = \sum_{\xi\in\Gamma} \varepsilon_{ij}^{s,\xi}(x, y, z), \tag{2.8}$$

where $\varepsilon_{ij}^{s,\xi}(x, y, z)$ is given by (2.7) and Γ denotes the set of jump points for $\overline{u}_1$.

Since the material is linear elastic, the strain energy density is a positive-definite continuous bilinear function of the actual strain fields $\varepsilon_{ij}(x, y, z)$, i.e. $\frac{1}{2}\mathbb{C}_{ijkl}\varepsilon_{ij}\varepsilon_{kl}$, where $\mathbb{C}_{ijkl}$ denotes the elasticity tensor. For convenience, we will indicate in the following with a $\overline{(\cdot)}$, as in (2.6), the mean value in the cross section. Since $\mathbb{C}_{ijkl} = \mathbb{C}_{klij}$, we can write from (2.1) and (2.8)

$$\begin{aligned}\frac{1}{2}\overline{\mathbb{C}_{ijkl}\varepsilon_{ij}\varepsilon_{kl}} \;=\; & \frac{1}{2}\overline{\mathbb{C}_{ijkl}\varepsilon_{ij}^0\varepsilon_{kl}^0} + \overline{\mathbb{C}_{ijkl}\left(\sum_{\xi\in\Gamma}\varepsilon_{ij}^{s,\xi}\right)\varepsilon_{kl}^0} \\ & + \frac{1}{2}\overline{\mathbb{C}_{ijkl}\left(\sum_{\xi\in\Gamma}\varepsilon_{ij}^{s,\xi}\right)\left(\sum_{\xi'\in\Gamma}\varepsilon_{kl}^{s,\xi'}\right)}.\end{aligned} \tag{2.9}$$

For homogeneous isotropic elastic bodies, $\mathbb{C}_{ijkl}$ takes the form

$$\mathbb{C}_{ijkl} = \lambda\delta_{ij}\delta_{kl} + 2\mu\delta_{ik}\delta_{jl}, \tag{2.10}$$

where λ and μ are Lamè's constants, related to the Young's modulus E and the Poisson's ratio ν by

$$E = \frac{\mu(3\lambda + 2\mu)}{\lambda + \mu}, \qquad \nu = \frac{\lambda}{2(\lambda + \mu)}. \tag{2.11}$$

In this case, recalling (2.2), the first term on the right-hand side of (2.9) reads

$$\overline{\mathbb{C}_{ijkl}\varepsilon^0_{ij}\varepsilon^0_{kl}} = \mathbb{C}_{ijkl}\overline{\varepsilon^0_{ij}\varepsilon^0_{kl}} = E(\varepsilon^0_{11})^2, \tag{2.12}$$

where $\varepsilon^0_{11} = \sigma_0/E$.

Passing to the second term in (2.9), we observe from (2.2) that $\varepsilon^0_{ij} = [(1+\nu)(\delta_{i1}\delta_{j1} - \nu\delta_{ij})]\varepsilon^0_{11}$. Thus, using (2.7), we obtain for a homogeneous isotropic body, for which (2.10) and (2.11) hold,

$$\begin{aligned}
&\overline{\mathbb{C}_{ijkl}\Bigg(\sum_{\zeta\in\Gamma}\varepsilon^{s,\xi}_{ij}\Bigg)\varepsilon^0_{kl}} \\
&\quad= \frac{1}{A}\int_\Omega \mathbb{C}_{ijkl}\Bigg(\int_\Omega \sum_{\xi\in\Gamma}[\overline{u}_1](\xi)G_{ij}\big[(y,z),(\eta,\zeta),x-\xi\big]f(\eta,\zeta)\,\mathrm{d}\eta\,\mathrm{d}\zeta\Bigg)\varepsilon^0_{kl}\,\mathrm{d}y\,\mathrm{d}z \\
&\quad= \sum_{\xi\in\Gamma}[\overline{u}_1](\xi)\frac{E\varepsilon^0_{11}}{A}\int_\Omega\int_\Omega G_{11}\big[(y,z),(\eta,\zeta),x-\xi\big]f(\eta,\zeta)\,\mathrm{d}\eta\,\mathrm{d}\zeta\,\mathrm{d}y\,\mathrm{d}z.
\end{aligned} \tag{2.13}$$

It is convenient to introduce a kernel $\rho(x-\xi)$ and a positive constant K such that

$$\frac{\rho(x-\xi)}{K} = \frac{1}{A}\int_\Omega\int_\Omega G_{11}\big[(y,z),(\eta,\zeta),x-\xi\big]f(\eta,\zeta)\,\mathrm{d}\eta\,\mathrm{d}\zeta\,\mathrm{d}y\,\mathrm{d}z, \tag{2.14}$$

where K is selected so that $\int_{-\infty}^{+\infty}\rho(x-\xi)\,\mathrm{d}x = 1$. Because of (2.14) we can write

$$\overline{\mathbb{C}_{ijkl}\Bigg(\sum_{\zeta\in\Gamma}\varepsilon^{s,\xi}_{ij}\Bigg)\varepsilon^0_{kl}} = \sum_{\xi\in\Gamma}[\overline{u}_1](\xi)E\varepsilon^0_{11}\frac{\rho(x-\xi)}{K}. \tag{2.15}$$

It may be useful to recall, in passing, that by De Saint-Venant's principle the measure of the support of $\rho(\cdot)$ is of the same order as the bar diameter.

Finally, for what the final term in (2.9) is concerned, we can write from (2.7)

$$\begin{aligned}
&\overline{\mathbb{C}_{ijkl}\Bigg(\sum_{\xi\in\Gamma}\varepsilon^{s,\xi}_{ij}\Bigg)\Bigg(\sum_{\xi'\in\Gamma}\varepsilon^{s,\xi'}_{kl}\Bigg)} \\
&\quad= \frac{1}{A}\mathbb{C}_{ijkl}\sum_{\xi\in\Gamma}\sum_{\xi'\in\Gamma}[\overline{u}_1](\xi)[\overline{u}_1](\xi')\int_\Omega\int_\Omega G_{ij}\big[(y,z),(\eta,\zeta),x-\xi\big] \\
&\qquad\times G_{kl}\big[(y,z),(\eta,\zeta),x-\xi'\big]f^2(\eta,\zeta)\,\mathrm{d}\eta\,\mathrm{d}\zeta\,\mathrm{d}y\,\mathrm{d}z.
\end{aligned} \tag{2.16}$$

We now imagine that the resulting cracks are at quite a distance the one from the other, i.e. $|\xi'-\xi| > D$, $\forall\xi,\xi'\in\Gamma$ with $\xi\neq\xi'$, where D is of the same order as the bar diameter. This assumption will be verified *a posteriori* later on, when we will find that minimizers of the energy functional resulting from this hypothesis, at least in the case of strong interaction (see Section 6), will indeed prescribe a certain minimum spacing between any two consecutive cracks. In short,

even neglecting in (2.16) the mixed terms containing $[\overline{u}_1](\xi)[\overline{u}_1](\xi')$ with $\xi \neq \xi'$, the interaction contribution given by (2.13) is sufficient to maintain the cracks sufficiently far apart. From De Saint-Venant's principle, we thus can write

$$\int_\Omega \int_\Omega G_{ij}\big[(y,z),(\eta,\zeta),x-\xi\big] G_{kl}\big[(y,z),(\eta,\zeta),x-\xi'\big] \times f^2(\eta,\zeta)\,\mathrm{d}\eta\,\mathrm{d}\zeta\,\mathrm{d}y\,\mathrm{d}z \cong 0 \quad \text{for } \xi \neq \xi', \tag{2.17}$$

and, consequently,

$$\begin{aligned}
&\overline{\mathbb{C}_{ijkl}\Big(\sum_{\xi\in\Gamma}\varepsilon_{ij}^{s,\xi}\Big)\Big(\sum_{\xi'\in\Gamma}\varepsilon_{kl}^{s,\xi'}\Big)} \\
&\quad\cong \frac{1}{A}\mathbb{C}_{ijkl}\sum_{\xi\in\Gamma}[\overline{u}_1]^2(\xi)\int_\Omega\int_\Omega G_{ij}\big[(y,z),(\eta,\zeta),x-\xi\big] \\
&\qquad\times G_{kl}\big[(y,z),(\eta,\zeta),x-\xi\big] f^2(\eta,\zeta)\,\mathrm{d}\eta\,\mathrm{d}\zeta\,\mathrm{d}y\,\mathrm{d}z \\
&\quad= E\sum_{\xi\in\Gamma}\left([\overline{u}_1](\xi)\frac{\hat\rho(x-\xi)}{\widehat{K}}\right)^2,
\end{aligned} \tag{2.18}$$

where $\hat\rho(\cdot)$ is a weight function, similar to that defined in (2.15), and $\widehat{K}$ is an appropriate constant. Recall that, again by De Saint-Venant's principle, the support of $\hat\rho(\cdot)$ is of the same order as the bar diameter.

Collecting all these results, we can write

$$\begin{aligned}
&\frac{1}{2}\overline{\mathbb{C}_{ijkl}\varepsilon_{ij}\varepsilon_{kl}} \\
&\quad= \frac{1}{2}E(\varepsilon_{11}^0)^2 + \sum_{\xi\in\Gamma}[\overline{u}_1](\xi)E\varepsilon_{11}^0\frac{\rho(x-\xi)}{K} + \frac{1}{2}E\sum_{\xi\in\Gamma}\left([\overline{u}_1](\xi)\frac{\hat\rho(x-\xi)}{\widehat{K}}\right)^2 \\
&\quad= \frac{1}{2}E\left[\varepsilon_{11}^0 + \sum_{\xi\in\Gamma}[\overline{u}_1](\xi)\frac{\rho(x-\xi)}{K_1}\right]^2 \\
&\qquad+ \frac{1}{2}E\sum_{\xi\in\Gamma}\left([\overline{u}_1](\xi)\frac{\hat\rho(x-\xi)}{\widehat{K}}\right)^2 - \frac{1}{2}E\left(\sum_{\xi\in\Gamma}[\overline{u}_1](\xi)\frac{\rho(x-\xi)}{K}\right)^2.
\end{aligned} \tag{2.19}$$

But, recall again that we have supposed the cracks sufficiently far apart one from the other and at a distance from the bar ends (see footnote ⋆ on page 6). We thus find, again by De Saint-Venant's principle, that

$$\int_{\mathcal{I}} \frac{1}{2} E \left\{ \sum_{\xi\in\Gamma} \left([\overline{u}_1](\xi) \frac{\hat{\rho}(x-\xi)}{\widehat{K}} \right)^2 - \left(\sum_{\xi\in\Gamma} [\overline{u}_1](\xi) \frac{\rho(x-\xi)}{K} \right)^2 \right\} \mathrm{d}x$$
$$\cong \sum_{\xi\in\Gamma} g\big([\overline{u}_1](\xi)\big), \tag{2.20}$$

where $g(\cdot)$ is quadratic. In other words, the assumption of sufficient spacing among the cracks allows one to neglect in (2.20) the mixed terms containing $[\overline{u}_1](\xi)[\overline{u}_1](\xi')$, $\forall \xi, \xi' \in \Gamma$ with $\xi \neq \xi'$.

The strain energy stored in the bar, defined as

$$\begin{aligned} \mathcal{E}_b &= \frac{1}{2} \int_{\mathcal{B}} \mathbb{C}_{ijkl} \varepsilon_{ij} \varepsilon_{kl} \, \mathrm{d}x \, \mathrm{d}y \, \mathrm{d}z = \frac{1}{2} \int_{\mathcal{I}} \left(\int_{\Omega} \mathbb{C}_{ijkl} \varepsilon_{ij} \varepsilon_{kl} \, \mathrm{d}y \, \mathrm{d}z \right) \mathrm{d}x \\ &= \frac{1}{2} A \int_{\mathcal{I}} \overline{\mathbb{C}_{ijkl} \varepsilon_{ij} \varepsilon_{kl}} \, \mathrm{d}x, \end{aligned}$$

from (2.12), (2.15), (2.18), (2.19) and (2.20) thus results

$$\mathcal{E}_b = \frac{1}{2} EA \int_{\mathcal{I}} \left(\varepsilon_{11}^0 + \sum_{\xi\in\Gamma} [\overline{u}_1](\xi) \frac{\rho(x-\xi)}{K_1} \right)^2 \mathrm{d}x + \sum_{\xi\in\Gamma} g\big([\overline{u}_1](\xi)\big). \tag{2.21}$$

To this expression, which represents the work necessary to deform the elastic portions in between the cracks (bulk energy), the work expended to overcome the intermolecular forces and physically open the crack must be added (fracture energy). In general, following [8], by introducing the molecular potential $\theta(\cdot)$ the fracture energy term can be written in the form

$$\mathcal{E}_f = \int_{\Omega} \theta\big([u_1](\xi, \eta, \zeta)\big) \, \mathrm{d}\eta \, \mathrm{d}\zeta, \tag{2.22}$$

or, recalling (2.5),

$$\mathcal{E}_f = \int_{\Omega} \theta\big(f(\eta, \zeta)[\overline{u}_1](\xi)\big) \, \mathrm{d}\eta \, \mathrm{d}\zeta = \Theta\big([\overline{u}_1](\xi)\big).$$

Consequently, defining $\varphi(\cdot)$ as

$$\varphi\big([\overline{u}_1](\xi)\big) = \Theta\big([\overline{u}_1](\xi)\big) + g\big([\overline{u}_1](\xi)\big), \tag{2.23}$$

we obtain for the total energy an expression of the type

$$\mathcal{E}[\overline{u}_1] = \frac{1}{2} EA \int_{\mathcal{I}} \left(\varepsilon_{11}^0 + \sum_{\xi\in\Gamma} [\overline{u}_1](\xi) \frac{\rho(x-\xi)}{K} \right)^2 \mathrm{d}x + \varphi\big([\overline{u}_1](\xi)\big). \tag{2.24}$$

In this expression, the kernel $\rho(\cdot)$ models the non-local effect produced by the elastic distortions that accompany the crack growth, whereas $\varphi(\cdot)$ is "apparently" the surface energy. Indeed, we deduce more accurately from (2.23), that $\varphi(\cdot)$ is the

sum of two contributions: the "true" fracture energy, $\Theta([\overline{u}_1](\xi))$, and the aliquot $g([\overline{u}_1](\xi))$, which results from the distortions produced at the crack surfaces.

3. The Variational Problem for a Hard Device

Motivated by the analysis of the previous section, we conceive one-dimensional models for tensile bars defined, in general, through deformation energies of the type

$$\Pi[u] := \int_{\mathcal{I}} U\left(u'(x) + \frac{1}{K}\sum_{x_i \in J_u} [u](x_i)\rho(x - x_i)\right) \mathrm{d}x + \sum_{x_i \in J_u} \varphi\big([u](x_i)\big). \quad (3.1)$$

Here, in the reference system x, the interval $\mathcal{I} \equiv [0, L] \subset \mathbb{R}$ denotes the bar natural undistorted reference-configuration, $u(x)$ is the displacement in the positive x direction of particles initially at x, $U\colon \mathbb{R} \to \mathbb{R}$ is a regular function representative of the bulk part of the energy, $\varphi\colon \mathbb{R}^+ \to \mathbb{R}$ is the "interfacial" term, J_u is the set of jump points of u and $[u](x_i)$ the jump of u at $x_i \in J_u$. The most important peculiarity of (3.1) is that the bulk energy is a function not only of the "regular" gradient u', but also of a non-local term defined by singular part $[u]$ and the kernel $\rho\colon \mathbb{R} \to \mathbb{R}$, a function identically zero outside the interval $(-l_0, l_0)$, with* $l_0 \ll L$. By appropriately defining the constant K we can always set

$$\int_{-l_0}^{l_0} \rho(t)\,\mathrm{d}t = 1. \quad (3.2)$$

Since discontinuous displacement fields are envisaged, the natural space where to settle the variational problem is the space of real valued functions of bounded variation $BV(\mathcal{I})$. The generalized derivative $\mathrm{D}u$ of u is a measure on $\mathcal{I}$ and, according to [1] (see also [2]), we can decompose $\mathrm{D}u$ in the form

$$\mathrm{D}u = u'_a + \mathrm{D}_c u + \mathrm{D}_j u = u'_a + \mathrm{D}_s u, \quad (3.3)$$

where u'_a, $\mathrm{D}_c u$ and $\mathrm{D}_j u$ denote the absolutely continuous part of $\mathrm{D}u$ with respect to the Lebesgue's measure $\mathrm{d}x$ (an equivalent notation for u'_a, sometimes used in this paper, is $\mathrm{D}_a u$), the Cantor part and the jump part of $\mathrm{D}u$, respectively. Consequently, $\mathrm{D}_s u = \mathrm{D}_c u + \mathrm{D}_j u$ represents the singular part of $\mathrm{D}u$ (with respect to the Lebesgue's measure $\mathrm{d}x$).

Notice that the convolution product is well defined also for singular functions. If we set $\mathrm{D}_j u(x) \equiv 0$ in the sense of distributions for $x \notin [0, L]$, we have in particular

$$(\rho * \mathrm{D}_j u)(x) = \int_{-\infty}^{+\infty} \rho(x - z)\mathrm{D}_j u(z) = \sum_{x_i \in J_u} [u](x_i)\rho(x - x_i). \quad (3.4)$$

* Recall again the key role played by De Saint-Venant's principle in Section 2.

Consequently, we can write (3.1) with a more convenient mathematical notation in the form

$$\Pi[u] := \int_{\mathcal{I}} U\left(u'_a + \frac{1}{K}\rho * \mathrm{D}_j u\right) \mathrm{d}x + \sum_{x_i \in J_u} \varphi\big([u](x_i)\big). \tag{3.5}$$

Suppose now that the bar is gradually stretched in a hard device so that its total length becomes $(\beta + 1)L$. Thus, the quantity $\beta \geqslant 0$ represents the average strain and $\mathrm{D}u$ must satisfy an integral condition of the form

$$\beta L = \int_{\mathcal{I}} \mathrm{D}u = \int_{\mathcal{I}} u'_a \,\mathrm{d}x + \int_{\mathcal{I}} \mathrm{D}_c u + \sum_{x_i \in J_u} [u](x_i). \tag{3.6}$$

We shall then consider the variational problem

$$\min_{u \in \mathcal{A}} \Pi[u], \tag{3.7}$$

consisting in minimizing the strain energy $\Pi[u]$ in the class $\mathcal{A}$ of admissible functions

$$\mathcal{A} = \left\{ u \in SBV(\mathcal{I})\colon\ u(0) = 0,\ \int_{\mathcal{I}} \mathrm{D}u = \beta L,\ \mathrm{D}u \geqslant \kappa \right\}. \tag{3.8}$$

It should be observed that $\mathcal{A}$ is a subset of the space of special bounded-variation functions SBV. We will demonstrate that for a wide choice of functions $U(\cdot)$ and $\varphi(\cdot)$, $\Pi[u]$ has a minimum in $\mathcal{A}$. However, it is important to mention that the integral condition $\int_{\mathcal{I}} \mathrm{D}u = \beta L$ and the lower bound $\mathrm{D}u \geqslant \kappa$ in (3.8), together, assure the boundedness of the class $\mathcal{A}$, which will be used in our proof. Indeed, without condition $\mathrm{D}u \geqslant \kappa$, we would be forced to assume more restrictive hypotheses on $\varphi(\cdot)$ in order to prove existence. From a physical point of view, we recall that for $\kappa = -1$ such lower bound expresses the injectivity condition for the deformation associated to u. In general, for the existence of minimizers it is sufficient to assume that $\mathrm{D}u$ is bounded from below.

4. Existence of Minimizers for the Variational Problem

We now address the question of the existence of minimizers for the variational problem presented in Section 3. In particular, we demonstrate the following:

THEOREM 1 (Existence of minimizers). *Let $U\colon \mathbb{R} \to \mathbb{R}$ and $\varphi\colon \mathbb{R}^+ \to \mathbb{R}$ be positive functions such that U is convex, φ is subadditive and, in addition,*

$$\lim_{t \to 0^+} \frac{\varphi(t)}{t} = +\infty, \tag{4.1}$$

and

$$\lim_{t \to +\infty} \frac{U(t)}{t} = +\infty. \tag{4.2}$$

Moreover, let $\rho(\cdot)$ be continuous and with compact support. Then the minimum problem defined in (3.7)*,* (3.5) *and* (3.8) *admits at least a solution.*

Before addressing the proof of the theorem, we notice that the class $\mathcal{A}$ is bounded in $BV(\mathcal{I})$. Indeed, let us choose any $u \in \mathcal{A}$. Then, its generalized derivative can be decomposed in the form $\mathrm{D}u = \mathrm{D}u^+ - \mathrm{D}u^-$, being $\mathrm{D}u^+$ and $(-\mathrm{D}u^-)$ the positive and the negative part of $\mathrm{D}u$. Since $\mathrm{D}u \geqslant \kappa$, we have $\int_{\mathcal{I}} \mathrm{D}u^- \leqslant |\kappa| L$ and, consequently,

$$\beta L = \int_{\mathcal{I}} \mathrm{D}u = \int_{\mathcal{I}} \mathrm{D}u^+ - \int_{\mathcal{I}} \mathrm{D}u^- \geqslant \int_{\mathcal{I}} \mathrm{D}u^+ - |\kappa| L.$$

Hence,

$$\int_{\mathcal{I}} |\mathrm{D}u| = \int_{\mathcal{I}} \mathrm{D}u^+ + \int_{\mathcal{I}} \mathrm{D}u^- \leqslant (\beta + |\kappa|)L + |\kappa| L,$$

which together with condition $u(0) = 0$ implies the boundedness of $\mathcal{A}$.

Proof. The proof of the theorem uses, with appropriate modifications, the ideas contained in a fundamental theorem by Ambrosio (Closure Theorem for *SBV* in [1]). Essentially, it consists in verifying that

(a) the functional $\Pi[u]$ defined in (3.5) is lower-semicontinuous in $\mathcal{A}$ for the weak* topology in $BV(\mathcal{I})$;

(b) for any sequence $(u_n) \subset \mathcal{A}$ that weakly* converges to some $u \notin \mathcal{A}$, we have

$$\lim_{n \to \infty} \Pi[u_n] = +\infty. \tag{4.3}$$

In fact, provided these two conditions hold, consider any minimizing sequence $(u_n) \subset \mathcal{A}$. Since $\mathcal{A}$ is bounded, its weak* closure $\overline{\mathcal{A}}$ is weakly* compact. Thus (u_n) converges, up to a subsequence, to some $u \in \overline{\mathcal{A}}$. But, because of condition (b), $u \in \mathcal{A}$ and, because of condition (a), $\Pi[u] \leqslant \liminf \Pi[u_n]$; we then conclude that u is a minimizer.

Since it is always possible to restate the variational problem defined in (3.7), (3.5) and (3.8) in term of the new function $\overline{u}(x) = u(x) - \kappa x$, without loosing generality, for the proof of (a) and (b) it is sufficient to consider the case $\kappa = 0$ in (3.8), so that from now on we consider $\mathrm{D}u \geqslant 0$.

We start by proving (a). Let $(u_n) \subset \mathcal{A}$ be a sequence weakly* – BV converging to some $u \in \mathcal{A}$. Then, there are only three possibilities:

(1) $\mathrm{D}_s u_n$ converges to a measure that is not singular;

(2) $\mathrm{D}_a u_n$ converges to a measure that is not absolutely continuous;

(3) $\mathrm{D}_s u_n$ converges to $\mathrm{D}_s u$ and $\mathrm{D}_a u_n$ converges to $\mathrm{D}_a u$.

In *case* 1 the sequence $(\mathrm{D}_s u_n)$ converges to a measure μ that is not singular with respect to the Lebesgue's measure, that is $\mu = \mu^{(1)} + \mu^{(2)}$ where $\mu^{(1)}$ is singular with respect to $\mathrm{d}x$ but $\mu^{(2)}$ is not vanishing and absolutely continuous (with respect to $\mathrm{d}x$). We can then split u_n into three terms, i.e. $u_n = u_n^{(0)} + u_n^{(1)} + u_n^{(2)}$ such that

$\mathrm{D}_s u_n^{(0)} = 0$, $\mathrm{D}_a u_n^{(1)} = \mathrm{D}_a u_n^{(2)} = 0$ and the sequence $(\mathrm{D}_s u_n^{(1)})$ converges to $\mu^{(1)}$ whereas $(\mathrm{D}_s u_n^{(2)})$ converges to $\mu^{(2)}$. Thus,

$$\liminf_{n\to\infty} \int_{\mathcal{I}} \mathrm{D}_s u_n^{(2)} \neq 0, \tag{4.4}$$

and

$$\lim_{n\to\infty} \sup_{x\in\mathcal{I}} \big[u_n^{(2)}\big](x) = 0. \tag{4.5}$$

Now, let us call $E_1^n \subset \mathcal{I}$ and $E_2^n \subset \mathcal{I}$ the sets where $\mathrm{D}_s u_n^{(1)}$ and $\mathrm{D}_s u_n^{(2)}$ are concentrated; expressions (4.4) and (4.5), together with (4.1) and (4.2) imply that

$$\lim_{n\to\infty} \sum_{x_i\in E_2^n} \varphi\big(\big[u_n^{(2)}\big](x_i)\big) = +\infty.$$

We also observe that, because of the singularity of $\mu^{(2)}$ with respect to $\mu^{(1)}$, we have

$$\lim_{n\to\infty} \int_{E_1^n} \big|\mathrm{D}_s u_n^{(2)}\big| = \lim_{n\to\infty} \int_{E_1^n} \mathrm{D}_s u_n^{(2)} = 0.$$

Consequently,

$$\begin{aligned}&\liminf_{n\to\infty} \sum_{x_i\in J_{u_n}} \varphi\big([u_n](x_i)\big)\\ &\quad= \liminf_{n\to\infty}\Bigg(\sum_{x_i\in E_1^n} \varphi\big(\big[u_n^{(1)}\big](x_i)\big) + \sum_{x_k\in E_2^n} \varphi\big(\big[u_n^{(1)}\big](x_k)\big)\Bigg) = +\infty.\end{aligned}$$

This implies the sequentially lower-semicontinuity of $\Pi[\cdot]$ for sequences of this type.

In *case* 2, the sequence $(\mathrm{D}_a u_n)$ converges to a measure that is not absolutely continuous with respect to $\mathrm{d}x$. We can now decompose u_n in the form $u_n = u_n^{(\alpha)} + u_n^{(\gamma)}$ where $\mathrm{D}_s u_n^{(\alpha)} = 0$ but $\mathrm{D}_a u_n^{(\alpha)}$ converges to a (positive) measure μ that is singular with respect to $\mathrm{d}x$. Then, defining for some $\lambda \in \mathbb{R}^+$ the set $E_\lambda^n \equiv \{x \in \mathcal{I}\colon \mathrm{D}_a u_n^{(\alpha)} \geqslant \lambda\}$, we have

$$\liminf_{n\to\infty} \int_{E_\lambda^n} \mathrm{D}_a u_n^{(\alpha)}\,\mathrm{d}x = \liminf_{n\to\infty} \int_{\mathcal{I}} \mathrm{D}_a u_n^{(\alpha)}\,\mathrm{d}x \geqslant \int_{\mathcal{I}} \mu > 0. \tag{4.6}$$

Thus, recalling that $U(\cdot)$ is bounded from below, that $\rho * \mathrm{D}_s u_n$ is equibounded in L^∞ and that $\mathrm{D}_a u_n = \mathrm{D}_a u_n^{(\alpha)} + \mathrm{D}_a u_n^{(\gamma)} \geqslant \mathrm{D}_a u_n^{(\alpha)}$ (since $\mathrm{D}_a u_n^{(\gamma)} \geqslant 0$), we obtain recalling (4.6)

$$\begin{aligned}\liminf_{n\to\infty} \int_{\mathcal{I}} U\bigg(\mathrm{D}_a u_n + \frac{1}{K}\rho * \mathrm{D}_s u_n\bigg)\,\mathrm{d}x \;&\geqslant\; \liminf_{n\to\infty} \int_{\mathcal{I}} U\big(\mathrm{D}_a u_n^{(\alpha)} + C_1\big)\,\mathrm{d}x\\ &\geqslant\; \liminf_{n\to\infty} \int_{E_\lambda^n} U\big(\mathrm{D}_a u_n^{(\alpha)} + C_1\big)\,\mathrm{d}x,\end{aligned} \tag{4.7}$$

for some constant C_1. But condition (4.2) implies that for every $A \in \mathbb{R}^+$ there is a λ such that

$$U\big(\mathrm{D}_a u_n^{(\alpha)}(x) + C_1\big) \geqslant A\big(\mathrm{D}_a u_n^{(\alpha)}(x) + C_1\big), \quad \forall x \in E_\lambda^n.$$

Using (4.6) and (4.7), we find

$$\liminf_{n\to\infty} \int_{E_\lambda^n} U\big(\mathrm{D}_a u_n^{(\alpha)} + C_1\big)\,\mathrm{d}x \geqslant \liminf_{n\to\infty} \int_{E_\lambda^n} A\big(\mathrm{D}_a u_n^{(\alpha)} + C_1\big)\,\mathrm{d}x \geqslant A \int_{\mathcal{I}} \mu.$$

Thus, from the arbitrariness of A, we obtain that $\liminf \Pi[u_n] \to +\infty$ as $n \to \infty$, from which the sequential lower-semicontinuity of $\Pi[\cdot]$ in case 2 follows.

Finally, in *case* 3, assume that the sequence $(\mathrm{D}_a u_n)$ converges to $\mathrm{D}_a u$ and $(\mathrm{D}_s u_n)$ converges to $\mathrm{D}_s u$. We recall that if a sequence of measures (μ_n) weakly*-converges to a measure μ, then $\rho * \mu_n$ converges strongly in L^1 to $\rho * \mu$ (this can be easily verified when ρ is of class C^1 by integrating by parts and can then be proved for a general ρ by approximating it with C^1 functions in the L^∞ norm). Consequently, we have that

$$\liminf_{n\to\infty} \int_{\mathcal{I}} U\left(\mathrm{D}_a u_n + \frac{1}{K}\rho * \mathrm{D}_s u_n\right)\mathrm{d}x \geqslant \int_{\mathcal{I}} U\left(\mathrm{D}_a u + \frac{1}{K}\rho * \mathrm{D}_s u\right)\mathrm{d}x. \tag{4.8}$$

Moreover, from the subadditivity hypothesis on $\varphi(\cdot)$ we conclude that (see for instance [2])

$$\liminf_{n\to\infty} \sum_{x_i \in J_{u_n}} \varphi\big([u_n](x_i)\big) \geqslant \sum_{x_i \in J_u} \varphi\big([u](x_i)\big). \tag{4.9}$$

From the exam of the three aforementioned cases, the sequential lower-semicontinuity of $\Pi[\cdot]$ in general follows and so condition (a) is satisfied.

We then pass to consider condition (b). Thus suppose that a sequence $(u_n) \subset \mathcal{A}$ weak*-BV converges to some u^*, with $u^* \in \overline{\mathcal{A}}$. Using arguments completely similar to those used in the discussion of cases 1 and 2, it can be shown that if $\mathrm{D}u^*$ has non-vanishing Cantor part, then

$$\liminf_{n\to\infty} \Pi[u_n] = +\infty. \tag{4.10}$$

In fact, if $\mathrm{D}_s u_n$ converges to a measure that has nonzero Cantor part, we can apply the argument of case 1; on the other hand, when $\mathrm{D}_a u_n$ converges to a measure with nonzero Cantor part, we may reason as in case 2. This concludes the proof of the theorem. □

5. Necessary Conditions for Minimizers

We now turn to the characterization of solutions of (3.7), by considering the first variation of the functional $\Pi[u]$. For simplicity, we will examine only the case

when $\kappa = 0$ in (3.8); the extension to the general case $\kappa \neq 0$ is more complicated but conceptually similar. Let then u^* be a minimizer for the variational problem (3.7). We consider variations of the form

$$u^* + \Delta u = u^* + \varepsilon v, \tag{5.1}$$

where v is a fixed function and ε is a small positive quantity, i.e. $\varepsilon > 0$. Obviously, because of the definition (3.8) of the class $\mathcal{A}$ of admissible functions, v must satisfy the integral condition

$$\int_{\mathcal{I}} \mathrm{D}v(x) = 0. \tag{5.2}$$

A necessary condition for u^* to be a minimizer is

$$\liminf_{\varepsilon \to 0^+} \frac{\Pi[u^* + \varepsilon v] - \Pi[u^*]}{\varepsilon} \geqslant 0, \tag{5.3}$$

and, in the following, we will specify this condition for particular choices of the function v. For convenience we will set

$$e^*(x) := \mathrm{D}_a u^*(x) + \frac{1}{K} \rho * \mathrm{D}_j u^*, \tag{5.4}$$

and define

$$\mathcal{I}_> := \left\{ x \in \mathcal{I} \colon \limsup_{\varepsilon \to 0} \frac{1}{2\varepsilon} \int_{x-\varepsilon}^{x+\varepsilon} \mathrm{D}_a u^* > 0 \right\}. \tag{5.5}$$

Then, the necessary conditions for minimizers are expressed by the following:

THEOREM 2 (Euler–Lagrange equations). *Let us suppose that u^* is a solution of the problem defined in* (3.7)*,* (3.5) *and* (3.8) *for $\kappa = 0$. Then the following conditions hold:*

(1)
$$U'\big(e^*(x)\big) = \text{const} = N_0 \quad \forall x \in \mathcal{I}_>,$$
and $U'(e^*(x)) \geqslant N_0$ $\forall x \in \mathcal{I} \backslash \mathcal{I}_>$;

(2) *if we denote by ρ^- the function $\rho^-(x) = \rho(-x)$ then*
$$\left(\frac{1}{K}\rho^- * U'(e^*)\right)(x_1) + \varphi'\big([u^*](x_1)\big) = \left(\frac{1}{K}\rho^- * U'(e^*)\right)(x_2) + \varphi'\big([u^*](x_2)\big),$$
for every $x_1, x_2 \in J_{u^*}$;

(3) *for every $x_1 \in J_{u^*}$ we have*
$$U'\big(e^*(x_1)\big) \geqslant \left(\frac{1}{K}\rho^- * U'(e^*)\right)(x_1) + \varphi'\big([u^*](x_1)\big) \quad \forall x_1 \in \mathcal{I} \backslash \mathcal{I}_>,$$
and equality holds if $x_1 \in \mathcal{I}_>$;

(4) *defining* $\overset{\circ}{J}_{u^*} = J_{u^*} \cap]0, L[$, *then*

$$\frac{\mathrm{d}}{\mathrm{d}x}\left[\frac{1}{K}\rho^- * U'(e^*)\right](x_1) = 0, \quad \forall x_1 \in \overset{\circ}{J}_{u^*};$$

if $x_1 = 0$ *the* sign $\geqslant$ *holds and if* $x_1 = L$ *the* sign $\leqslant$ *holds.*

Proof. Case 1. Consider in (5.1) $\Delta u = \varepsilon v_\eta(x)$ such that $\mathrm{D}v_\eta = \mathrm{D}_a v_\eta$, $\mathrm{D}_s v_\eta = 0$ and v_η weakly* converges in BV to a step function jumping at $x = x_1$ ($\mathrm{D}v_\eta$ converges to a Dirac's mass centered at x_1). Clearly, if $x_1 \in \mathcal{I}_>$ two sided variations are allowed for appropriate v_η and for sufficiently small ε, whereas if $x \in \mathcal{I}\backslash\mathcal{I}_>$ only one-sided variation is allowed. From (5.3) we obtain conditions

$$U'\big(e^*(x)\big) = \text{const} = N_0 \quad \forall x \in \mathcal{I}_>, \tag{5.6}$$

and

$$U'\big(e^*(x)\big) \geqslant N_0 \quad \forall x \in \mathcal{I}\backslash\mathcal{I}_>. \tag{5.7}$$

Case 2. Assuming that u^* has at least two points of discontinuity, consider now $\Delta u = \varepsilon v_2(x)$ where $v_2(x)$ is such that $\mathrm{D}v_2 = \delta_{x_1} - \delta_{x_2}$. Here δ_{x_1} and δ_{x_2} denote Dirac's masses centered at x_1 and x_2 respectively, where x_1 and x_2 are two distinct jump points for u^*. Since now two-sided variations are allowed, from (5.3) we obtain

$$\int_{\mathcal{I}}\left(\frac{1}{K}\rho * (\delta_{x_1} - \delta_{x_2})\right)U'(e^*)\,\mathrm{d}x + \varphi'\big([u^*](x_1)\big) - \varphi'\big([u^*](x_2)\big) = 0.$$

Thus, recalling the well-known formula

$$\int_{\mathcal{I}}\left(\frac{1}{K}\rho * (\delta_{x_1} - \delta_{x_2})\right)U'(e^*)\,\mathrm{d}x = \int_{\mathcal{I}}\left(\frac{1}{K}\rho^- * U'(e^*)\right)(\delta_{x_1} - \delta_{x_2})\,\mathrm{d}x,$$

where

$$\rho^-(x) = \rho(-x),$$

we find

$$\begin{aligned}&\left(\frac{1}{K}\rho^- * U'(e^*)\right)(x_1) + \varphi'\big([u^*](x_1)\big)\\ &\quad = \left(\frac{1}{K}\rho^- * U'(e^*)\right)(x_2) + \varphi'\big([u^*](x_2)\big),\end{aligned} \tag{5.8}$$

for every x_1, x_2 in J_{u^*}.

Case 3. Supposing that u^* has at least one discontinuity point, let $\mathrm{D}\Delta u = \varepsilon v_\eta'(x) - \varepsilon\delta_{x_2}$, where x_2 is a jump point for u^* and $v_\eta(x)$ has been defined as

in case 1 but with unit average, so that (5.2) is automatically satisfied. From (5.3) we find

$$\int_{\mathcal{I}} U'(e^*)\left(v'_\eta(x) - \frac{1}{K}\rho * \delta_{x_2}\right) \mathrm{d}x - \varphi'\big([u^*](x_2)\big) \geqslant 0.$$

As $v'_\eta(x) \rightharpoonup \delta_{x_1}$ for $\eta \to \infty$, we distinguish again the cases when $x_1 \in \mathcal{I}_>$ and when $x_1 \notin \mathcal{I}_>$. If $x_1 \in \mathcal{I}_>$ two sided variations are allowed, so that we obtain

$$U'\big(e^*(x_1)\big) = \left(\frac{1}{K}\rho^- * U'(e^*)\right)(x_2) + \varphi'\big([u^*](x_2)\big) \quad \forall x_1 \in \mathcal{I}_>, \tag{5.9}$$

whereas if $x \notin \mathcal{I}_>$ we find

$$U'\big(e^*(x_1)\big) \geqslant \left(\frac{1}{K}\rho^- * U'(e^*)\right)(x_2) + \varphi'\big([u^*](x_2)\big) \quad \forall x_1 \in \mathcal{I}\backslash\mathcal{I}_>. \tag{5.10}$$

Case 4. Finally, assuming again that there exists at least one jump point x_1 for u^*, consider variations Δu such that $\mathrm{D}\Delta u = [u^*](x_1)\delta_{x_1+\varepsilon} - [u^*](x_1)\delta_{x_1}$. This is equivalent to perturbing the position of the jump point from x_1 to $x_1 + \varepsilon$. If x_1 is sufficiently far from the extremities of the bar, we obtain from (5.3)

$$\begin{aligned}\int_{\mathcal{I}} U'(e^*)\left(\frac{1}{K}\rho * \delta'_{x_1}\right) \mathrm{d}x \;&=\; \int_{\mathcal{I}} \frac{1}{K}\rho^- * U'(e^*)\delta'_{x_1}\,\mathrm{d}x \\ &=\; -\int_0^L \frac{\mathrm{d}}{\mathrm{d}x}\left[\frac{1}{K}\rho^- * U'(e^*)\right]\delta_{x_1}\,\mathrm{d}x = 0,\end{aligned}$$

which implies

$$\frac{\mathrm{d}}{\mathrm{d}x}\left[\frac{1}{K}\rho^- * U'(e^*)\right](x_1) = 0 \quad \forall x_1 \in \overset{\circ}{J}_{u^*}. \tag{5.11}$$

If instead the jump point coincides with the lower extremity of the bar, i.e. $x_1 \equiv 0$, analogously to condition (5.11) we find

$$\frac{\mathrm{d}}{\mathrm{d}x}\left[\frac{1}{K}\rho^- * U'(e^*)\right](x_1) \geqslant 0 \quad \text{if } x_1 \equiv 0. \tag{5.12}$$

On the other hand when $x_1 \equiv L$ we obtain

$$\frac{\mathrm{d}}{\mathrm{d}x}\left[\frac{1}{K}\rho^- * U'(e^*)\right](x_1) \leqslant 0 \quad \text{if } x_1 \equiv L. \tag{5.13}$$

This concludes the proof of the theorem. □

6. The Shape of Minimizers. Discussion

As the value of the bar average strain β, characterizing the class (3.8) of admissible functions, is gradually increased starting from $\beta = 0$, the shape of minimizers for

the problem defined in (3.7) and (3.5) may correspondingly be different in type. Intuitively, the bar prefers to be uniformly stretched when β is moderate, whereas, for larger values, discontinuous deformations may be energetically more favorable. Optimal values for jumps are expected since, two competing terms appear in the energy expression (3.5): the surface energy $\varphi(\cdot)$, which because of (4.1) penalizes small discontinuities, and the bulk energy $U(\cdot)$ that, being a function of the convolution term $\rho * \mathrm{D}_j u$, is by (4.2) superlinear in the jump amount. The crucial question to be addressed now is whether the presence of the non-local term $\rho * \mathrm{D}_j u$ can possibly predict, or at least restrict, the jump position, that in models of the type (1.1) remains completely arbitrary.

Of course, different in type materials could be described for various choices of the bulk and surface energies $U(\cdot)$ and $\varphi(\cdot)$ and of the kernel $\rho(\cdot)$. Here, in addition to the hypotheses of Theorems 1 and 2, we will limit to discuss the paradigmatic example where $U(\cdot)$ is quadratic, $\varphi(\cdot)$ is strictly concave and $\rho(\cdot)$ is positive, symmetric and unimodal.* In particular, we consider the expressions

$$U(t) = \frac{1}{2} EAt^2, \qquad \varphi(t) = 2EAa\sqrt{\frac{K-1}{K}\frac{t}{L}}, \tag{6.1}$$

where E and A denote the Young's modulus and the cross section of the bar respectively, while a is a material parameter having the dimensions of a length.

But before proceeding further, it is important to review the boundary conditions at the bar ends, an issue that has been postponed up to now in order to simplify the presentation. In general (see also [13]), the non-local spatial dependence protrudes outside the reference domain when the non-local term is evaluated close to the boundary, so that an "extension" of deformation should be somehow defined beyond the frontier. In general, it is assumed that the deformation gradient vanishes outside the reference domain, but this choice may drastically affect the shape of minimizers. Referring to our model to illustrate, we can easily check that if we set $\mathrm{D}u \equiv 0$ outside the reference interval $\mathcal{I}$, it is energetically more convenient to nucleate a jump point in proximity of one of the bar extremities instead of in the interior of $\mathcal{I}$. In fact, supposing on the contrary that this is not the case, we can move the jump point to the border while maintaining fixed the jump amount. Since now only "half" of the convolution term is active, it could be easily checked that this second configuration, after a re-arrangement of $\mathrm{D}_a u$, lowers the energy. Similarly, a succeeding jump should be located at the second end-point.

Here, however, we prefer not to consider this boundary effect, essentially because we believe that the bar end conditions deserve a deeper attention, which goes beyond the aim of this paper. Indeed, while attempting to reproduce real experiments on tensile bars, it is not clear what a realistic condition should be at the extremities, where substantial portions are subjected to the action of the clamping

* That is, $\rho(\cdot)$ has only one maximum point, being increasing on the left-hand side and decreasing on the right-hand side of such point. An example is the function $\rho(t)$ defined as $\rho(t) = 3/(4l_0) \times (l_0^2 - t^2)$ for $t \in (-l_0, l_0)$, $\rho(t) = 0$ otherwise.

device. For example, slipping may occur between specimen and clamping jaws, so that the assumption $\mathrm{D}u \equiv 0$ outside $\mathcal{I}$ may lead to erroneous estimates. This point is crucial since, as just noticed for our model, slightly different boundary conditions may produce substantially different responses. This is why, at least at this stage, we prefer to set such a difficulty aside. To this aim, we might think, for example, that the bar is a circular ring wound on a drum of radius R. Supposing that a device allows to continuously increase R, the average elongation of the ring would be consequently augmented. Provided R is so large that the second order strains due to the bar curvature are negligible and assuming no friction, the total energy of the ring can still be represented by a functional of the type (3.5), where now $L = 2\pi R$. From a mathematical point of view, this is equivalent to minimizing the energy functional $\Pi[u]$ of (3.5) in the class

$$\mathcal{A}_p = \left\{ u \in SBV_{loc}(\mathbb{R}):\ u(0) = 0,\ \int_{\mathcal{I}} \mathrm{D}u = \beta L,\ \mathrm{D}u \geqslant 0,\ u \text{ is } L\text{-periodic} \right\}. \tag{6.2}$$

The conclusions of Theorems 1 and 2 remain valid even in this case and the corresponding proofs are substantially the same as in Sections 4 and 5. However now, because of the symmetry of the circular bar, no boundary effect is present and, by a proper translation of $\mathcal{I}$, we may always suppose that any jump occurs in the interior of the reference interval.

In this context, let us now qualitatively discuss the main characteristics of minimizers for different values of the average elongation β. As a matter of fact, explicit analytical solutions are very difficult to obtain and this is why, here, we limit to investigate only some qualitative properties of minimizers, whereas a more detailed numerical analysis for some particular cases will be presented in a forthcoming paper. Let's then analyze the informations achievable from the Euler–Lagrange equations (Section 5). First of all, whenever the deformation is continuous ($\mathrm{D}_j u^* = 0$), we find from condition 1 in Theorem 2 that the only possible equilibrium configuration corresponds to $\mathrm{D}_a u^* = \text{const} = \beta$. We can easily show that this is a minimum point for sufficiently small β. In fact, comparing the functional $\Pi[u]$ of (3.5) with

$$\widehat{\Pi}[u] = \int_{\mathcal{I}} U\big(u'_a(x)\big)\,\mathrm{d}x + \sum_{x_i \in J_u} \varphi\big([u](x_i)\big), \tag{6.3}$$

from the hypothesis $\mathrm{D}u \geqslant 0$ we certainly have $\widehat{\Pi}[u] \leqslant \Pi[u]$ in $\mathcal{A}$ and, besides, $\Pi[u] \equiv \widehat{\Pi}[u]$ if $\mathrm{D}_j u = 0$. We know (compare [10]), that for small values of β minimizers of $\widehat{\Pi}[u]$ have no singular part. Let then $\hat{u}^*$ be a *continuous* minimizer for $\widehat{\Pi}[u]$. Since we can write

$$\Pi\big[\hat{u}^*\big] = \widehat{\Pi}[\hat{u}^*] \leqslant \widehat{\Pi}[u] \leqslant \Pi[u], \quad \forall u \in \mathcal{A},$$

we find that $\hat{u}^*$ also minimizes $\Pi[u]$.

The situation is more complicated when β is augmented beyond a threshold value, corresponding to the appearance of discontinuities. Now a few cases have to be considered and, in particular, we have to distinguish two possibilities: either the jump occurs in the region $\mathcal{I}_>$, where according to (5.5) $\mathrm{D}_a u^* > 0$, or the jump occurs in the remaining part $\mathcal{I}\backslash\mathcal{I}_>$, where $\mathrm{D}_a u^*(x) = 0$.

(a) If a jump arises in $\mathcal{I}_>$, we find from condition 1 of Theorem 2 that $e^*(x) = \text{const} = e_0$, where e^* is defined by (5.4) and $e_0 = N_0/EA$. Thinking of decomposing $e^*(x)$ in the form $e^*(x) = \mathrm{D}_a u^* + e_J^*(x)$, where $e_J^*(x)$ represents the contribution due to the convolution terms, i.e.

$$e_J^*(x) = \sum_{x_j \in J_u} \frac{1}{K} \rho * \mathrm{D}_j u^*(x_j), \tag{6.4}$$

we find that the following condition holds:

$$e_J^*(x) < e_0, \quad \forall x \in \mathcal{I}_>.$$

This situation is evidenced on the left-hand side of Figure 2, where the graphs of $e^*(x)$ and $e_J^*(x)$ are represented with continuous and dotted lines, respectively. Moreover, noticing that condition 2 of Theorem 2 implies that $\varphi'([u](x_1)) = \varphi'([u](x_2))$ for every $x_1, x_2 \in J_{u^*} \cap \mathcal{I}_>$ (provided that the distance between x_i and the boundary points of $\mathcal{I}_>$ is big enough, i.e. greater than l_0), the strict concavity of φ gives that $[u](x_1) = [u](x_2)$, i.e. all the jumps must be of the same amount.

(b) For a jump located in $\mathcal{I}\backslash\mathcal{I}_>$, we have from condition 1 of Theorem 2 that $e^*(x) \geqslant e_0$. Then, using condition 3, we obtain the characterization

$$e_J^*(x) = e^*(x) \geqslant e_0, \quad \forall x \in \mathcal{I}\backslash\mathcal{I}_>,$$

which is illustrated by the corresponding graphs represented on the right-hand side of Figure 2.

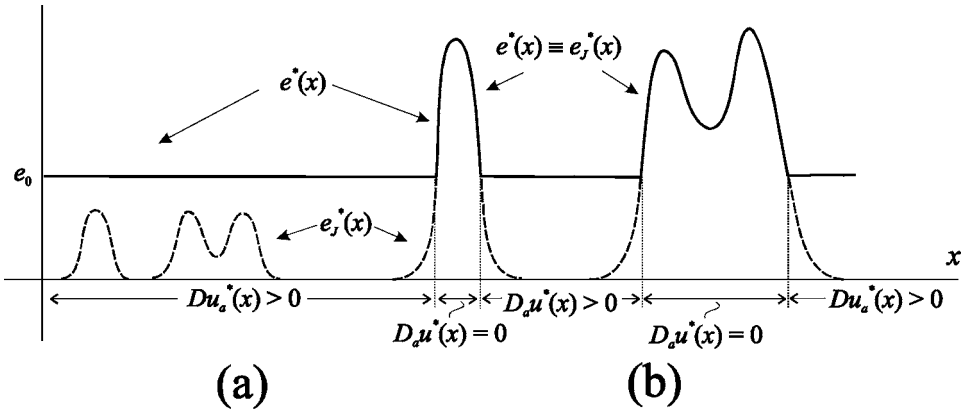

Figure 2. The two different configurations for minimizers: (a) $D_a u^*(x) > 0$ and $e_J^*(x) < e_0$; (b) $e^*(x) \equiv e_J^*(x)$ and $e_J^* \geqslant e_0$ where $D_a u^*(x) = 0$.

In conclusion, e^* is constant in $\mathcal{I}_>$ and greater than or equal to this value in $\mathcal{I}\backslash\mathcal{I}_>$. When more then one jump is present, the corresponding amounts must satisfy condition 2 of Theorem 2.

We may decide if the bar naturally prefers discontinuities either of the type (a) or of the type (b) by considering only one jump point. For this configuration, we can in principle easily determine, for fixed β, the optimal jump amount so as to minimize the total energy, but the calculations are lengthy and, therefore, we report them in the Appendix. In summary, the situation depends upon the value of the parameter α defined as

$$\alpha = \frac{K-1}{\rho_{\max} L + K - 1}, \tag{6.5}$$

where $\rho_{\max}$ denotes the maximum value of $\rho(\cdot)$. In particular, three different cases have to be analyzed according to whether $0 < \alpha < \frac{1}{3}$ or $\frac{1}{3} < \alpha < \frac{2}{3}$ or $\alpha > \frac{2}{3}$, but the borderline cases of practical interest are essentially only two: that of *strong interaction* and that of very *weak interaction*. Such possibilities, as the name suggests, depend upon the value of the parameter K, which controls the "strength" of the non-local term in (3.5).

In the case of very weak interaction, i.e. when K is very large ($K \gg \rho_{\max} L$), we have $\alpha \simeq 1$. Reasoning as in the Appendix, there exists a threshold value for β, say $\beta = \overline{\beta}$ such that for $\beta < \overline{\beta}$ the bar is uniformly strained (i.e. $\mathrm{D}_a u^* \equiv \beta$, $\mathrm{D}_j u^* \equiv 0$), whereas for $\beta > \overline{\beta}$ the situation with one jump of definite amount is energetically more favorable. The optimal jump amount, provided K is sufficiently large, satisfies condition $e^*_J(x) < e^*(x)$ with $e^*(x) = e_0$, so that the configuration is of the type (a).

We now consider the case of strong interaction, i.e. when $1 < K \ll \rho_{\max} L$. This situation is likely to be the most common in the practical cases because, noticing that since $\int \rho \, \mathrm{d}x = 1$ we certainly have $\rho_{\max} 2l_0 \geqslant 1$, from the hypothesis $L \gg l_0$ we find that, for a wide range of values of K, condition $K \ll \rho_{\max} L$ is certainly satisfied. In particular, whenever $K < 1 + \frac{1}{2}\rho_{\max} L$, we have $0 < \alpha < \frac{1}{3}$. Then, following the calculations in the Appendix, we can define the threshold value

$$\beta_3 = \frac{1}{\alpha}\left(\frac{a(K-1)}{\rho_{\max} L^2}\right)^{2/3},$$

such that (i) for $\beta < \beta_3$ the continuous deformation with $\mathrm{D}_a u^* \equiv \beta$ and $\mathrm{D}_j u^* \equiv 0$ is energetically favorable; (ii) for $\beta > \beta_3$ the configuration with one finite jump is to be preferred. Now however, on the contrary to the previous case, we find that the optimal jump $[u^*]$ verifies $(1/K)\rho_{\max}[u^*] > e^*_0$, i.e. the bar configuration is now of the type (b).

Let us then pass to the most interesting issue: what is the mutual influence between two cracks? The situation is quite different for the two aforementioned cases of weak or strong interaction. Let us consider first the case of weak interaction and consequently let $x_1, x_2 \in J_{u^*} \cap \mathcal{I}_>$. We show that the model does not restrict

the relative position of x_1 and x_2. In fact, supposing that x_1 and x_2 are moved arbitrarily close to one another in the interior of $\mathcal{I}_>$ where $e^*(x) = e_0$, we can always* rearrange $\mathrm{D}_a u^*$ so that $e^*(x)$ still remains equal to e_0 in $\mathcal{I}_>$. It is easily verified that in this way the energy level remains unchanged. Complete overlapping would lead to a different energy value because two jumps would merge into a larger one, thus affecting the term $\varphi(\cdot)$, but apart from this any two jumps could be placed as close as we like. This is not surprising, since the interaction due to the non-local term $\rho * \mathrm{D}_j u$ disappears for large K. In the limit case $K \to \infty$, the functional (3.5) reduces to (6.3), for which we had already noticed the complete freedom of movement for the jump points.

The scenario is quite different for strong interaction, i.e., we can demonstrate that the location of the jump points cannot be completely arbitrary. Indeed, we see that when two jumps appear, we are free to move one with respect to the other, but their overlapping is restricted. To illustrate, suppose $x_1, x_2 \in J_{u^*} \backslash \mathcal{I}_>$: whenever $|x_1 - x_2| < l_0$, we can easily verify that condition 4 of Theorem 2 cannot be verified. More generally, if the total number of jumps in $J_{u^*} \backslash \mathcal{I}_>$ is less than $L/l_0 - 1$, then overlapping is similarly restricted. In fact, suppose by contradiction that this is not the case. Then there exists a jump point $y \in J_{u^*} \backslash \mathcal{I}_>$ such that the following (or a symmetric situation) occurs: $J_{u^*} \cap (y, y + 2l_0) = 0$ and $J_{u^*} \cap (y - l_0, y) \neq 0$. Then, condition 4 of Theorem 2 would be violated at y. Moreover, from this fact we have that, for any $x_j \in J_{u^*}$, the quantity $((1/K)\rho^- * U'(e^*))(x_j)$ depends only on the height of the jump at x_j. Therefore condition 2 in Theorem 2 can be written in the form $F([u](x_j)) = F([u](x_k))$ for every $x_j, x_k \in J_{u^*}$, where $F(\cdot)$ depends upon the shape of U, φ and ρ. From this condition, apart from pathological cases, we find that the height of the jumps is forced to assume at most only a finite number of values.

As a matter of fact, the case of weak interaction should be considered a borderline case, where model (1.2) looses most of its significance. The reason for this can be seen just referring to the paradigmatic example of Section 2. In particular, recall that in (2.16) we neglected the mixed terms containing $[\overline{u}_1](\xi)[\overline{u}_1](\xi')$, $\xi \neq \xi'$, since we assumed, modulo a verification *a posteriori*, that the bar cracks were sufficiently distant. This hypothesis is reasonable for the case of strong interaction, when the first-order "interference" between the bar axial strain and the distortion produced at a crack, interpreted by (2.13), is effective enough to maintain cracks sufficiently far apart. But the hypothesis fails when the interaction is weak. In this latter case, the strain energy functional (1.2) should be enriched by the mixed terms in (2.16), representative of direct interactions among the cracks. This additional contribution should provide certain restrictions and limit the possible jump locations, but the discussion of this circumstance necessitates consideration of a new energy functional and we will not do this.

In summary, in the only significant case of strong interaction (K sufficiently small), the presence of the non-local term $(1/K)\rho * \mathrm{D}_j u$ in the argument of the bulk

* At least until the corresponding new value of $e_J^*(x)$, defined in (6.4), does not exceed e_0.

energy $U(\cdot)$ provides restrictions upon the relative position between consecutive jumps of minimizers, in agreement with the experimental evidence discussed at length in the Introduction. The analysis also shows that the field $e^*(\cdot)$, defined as in (5.4), is affected by the appearance of possible discontinuities. More in detail, the graph of $e^*(\cdot)$ shows a "bump" of the type represented on the right-hand side of Figure 2 in a neighborhood of any discontinuity point, becoming constant only at a distance of the same order as the support of ρ. We observe in passing that the resulting shape of $e^*(\cdot)$ is similar to the strain field measured in the proximity of a major crack in quasi-brittle materials, in a region usually referred to as the "process zone" [6]. It is also worth mentioning that energy minimizers are different in type for different values of the average elongation β. For small βs, the uniformly-deformed state minimizes the energy, but as β is augmented, discontinuities appear. Although a correlation still needs to be established between such mesoscopic transition and the bar gross response (this will be the subject of further research), we observe that when a discontinuity point appears, the bar is released. Consequently, the axial force diminishes, which is remindful of the well-known phenomenon of serrated deformation at yielding in metallic bars, usually referred to as the Portevin–Le Chatelier effect (see [14, 15]).

Of course the specific case here considered is far from being exhaustive of the potentiality of the model. Apart from the possibility of varying U and φ in (3.5), we believe that by simply modifying the shape of the kernel ρ, a wide variety of material behaviors could be described. In particular, the case when ρ presents both negative and positive parts should furnish more precise restriction on the position of the discontinuity points throughout the bar, possibly reproducing with great accuracy the surprising order evidenced in Figure 1.

Acknowledgements

G.R. would like to express his most grateful appreciation to Professor Hans Weinberger for extremely helpful discussion during the preparation of this work. Partial support of the City of Helsinki and of the European Community under Mara Project is gratefully acknowledged.

Appendix A. The Case of One Jump Point

Suppose that the minimizing displacement field $u^*(x)$ has, at most, one jump point at, say, $x = x_1$. When $\rho(\cdot)$ is positive, symmetric and unimodal and, as in (6.1),

$$U(t) = \frac{1}{2}EAt^2, \qquad \varphi(t) = 2EAa\sqrt{\frac{K-1}{K}}\frac{t}{L},$$

recalling the necessary conditions of Section 5 and the discussion of Section 6, we find that there are only two possibilities to be considered. Defining, as in (5.4), $e^*(x) := \mathrm{D}_a u^*(x) + (1/K)\rho * \mathrm{D}_j u^*$, then either:

(1) $e^*(x) = e_0$ is constant in the bar,
(2) or $e^*(x) = e_0$ is constant in the bar except in the open interval $|x - x_1| < \Delta$, where $e^*(x) = (1/K)[u^*](x_1)\rho(x - x_1) > e_0$.

Case 1. If $e = \text{const} = e_0$, then

$$\mathrm{D}_a u^*(x) = e_0 - [u^*](x_1)\frac{\rho(x - x_1)}{K} \geqslant 0. \tag{A.1}$$

Since $\int \rho \, \mathrm{d}x = 1$, the integral condition (3.6) states that

$$e_0 L - \frac{1}{K}[u^*](x_1) = \beta L - [u^*](x_1) \tag{A.2}$$

so that

$$e_0 = \beta - \frac{K-1}{KL}[u^*](x_1).$$

Thus from inequality (A.1) we obtain the condition

$$[u^*](x_1) \leqslant \frac{K\beta L}{\rho_{\max} L + K - 1}. \tag{A.3}$$

Using (A.2) in the expression of the energy, we need to minimize

$$\begin{aligned} \mathcal{F}\big([u^*](x_1)\big) &= \int_0^L U\left(\beta - \frac{K-1}{KL}[u^*](x_1)\right) + \varphi\big([u^*](x_1)\big) \\ &= \frac{1}{2}EAL\left(\beta - \frac{K-1}{KL}[u^*](x_1)\right)^2 + 2EAa\sqrt{\frac{K-1}{KL}[u^*](x_1)}, \end{aligned} \tag{A.4}$$

for $[u^*](x_1)$ subjected to the inequality (A.3). It is convenient to define the variable p as

$$p := \sqrt{\frac{K-1}{KL}[u^*](x_1)}. \tag{A.5}$$

With this choice the problem becomes that of minimizing, for given β, the function

$$f(p) = \frac{1}{2}EAL\big(\beta - p^2\big)^2 + 2EAap, \tag{A.6}$$

subject to the constraint, deriving from (A.3),

$$p \leqslant \sqrt{\alpha\beta},$$

where, from (A.5),

$$\alpha = \frac{K-1}{\rho_{\max} L + K - 1}. \tag{A.7}$$

Differentiation of (A.6) with respect to p gives

$$f'(p) = 2EA(p^3L - \beta pL + a), \tag{A.8}$$
$$f''(p) = 2EAL(3p^2 - \beta). \tag{A.9}$$

At the upper bound $p = \sqrt{\alpha\beta}$ we have

$$f(\sqrt{\alpha\beta}) = f(0) + \frac{1}{2}EA\sqrt{\alpha\beta}\big[4a - \beta\sqrt{\alpha\beta}(2-\alpha)L\big], \tag{A.10}$$
$$f'(\sqrt{\alpha\beta}) = 2EA\big[a - \beta\sqrt{\alpha\beta}(1-\alpha)L\big], \tag{A.11}$$
$$f''(\sqrt{\alpha\beta}) = 2EAL\beta(3\alpha - 1). \tag{A.12}$$

Moreover, we notice from (A.7) that, since $K \geqslant 1$, we have $0 < \alpha < 1$. For convenience, we also introduce the quantities

$$\beta_1 = \left(\frac{a/L}{\alpha^{1/2}(1-\alpha)}\right)^{2/3}, \qquad \beta_2 = \left(\frac{4a/L}{\alpha^{1/2}(2-\alpha)}\right)^{2/3}. \tag{A.13}$$

We now need to distinguish three subcases.

Case 1a. Suppose that $K < 1 + \frac{1}{2}\rho_{\max}L$ so that $\alpha < \frac{1}{3}$. In this case, from (A.13), we have also $\beta_1 < \beta_2$. From (A.9) $f(p)$ is concave in the interval of definition $0 < p < \sqrt{\alpha\beta}$, and we observe from (A.8) that $f'(0) > 0$. Moreover, from (A.10), (A.11) and (A.12), it is easy to verify that when $0 < \beta < \beta_1$ we have $f(\sqrt{\alpha\beta}) > f(0)$ and $f'(\sqrt{\alpha\beta}) > 0$. When instead $\beta_1 < \beta < \beta_2$, $f(\sqrt{\alpha\beta}) > f(0)$ but $f'(\sqrt{\alpha\beta}) < 0$. Finally, when $\beta > \beta_2$ we obtain $f(\sqrt{\alpha\beta}) < f(0)$ but $f'(\sqrt{\alpha\beta}) < 0$. The corresponding graphs of $f(p) - f(0)$ are represented in Figure 3 as a function of p. We deduce that if $\alpha < \frac{1}{3}$, for $\beta < \beta_2$, the most convenient situation is when $p = 0$ (no jump). When instead $\beta > \beta_2$, the situation of interest is at the other extremum, i.e. $p = \sqrt{\alpha\beta}$, to which, from (A.7), corresponds a jump of amount $[u^*](x_1) = KL\beta/(\rho_{\max}L + K - 1)$.

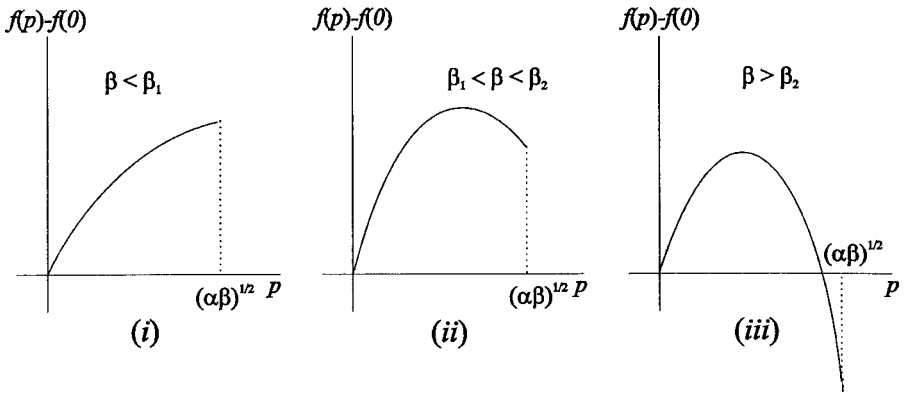

Figure 3. Graphs of $f(p) - f(0)$ for (i) $0 < \beta < \beta_1$, (ii) $\beta_1 < \beta < \beta_2$ and (iii) $\beta > \beta_2$. Case $\alpha < 1/3$.

Case 1b. When $1 + \frac{1}{2}\rho_{\max}L < K < 1 + 2\rho_{\max}L$ so that $\frac{1}{3} < \alpha < \frac{2}{3}$, again we have $\beta_1 < \beta_2$, but now from (A.9) $f(p)$ is concave for $0 < p < \sqrt{1/3}$ and convex for $\sqrt{1/3} < p < \sqrt{\alpha\beta}$. Again $f'(0) > 0$ and, from (A.10), (A.11) and (A.12), when $0 < \beta < \beta_1$ we have $f(\sqrt{\alpha\beta}) > f(0)$ and $f'(\sqrt{\alpha\beta}) > 0$; when $\beta_1 < \beta < \beta_2$, $f(\sqrt{\alpha\beta}) > f(0)$ and $f'(\sqrt{\alpha\beta}) < 0$; when $\beta > \beta_2$ we obtain $f(\sqrt{\alpha\beta}) < f(0)$ but $f'(\sqrt{\alpha\beta}) < 0$. The graphs of $f(p) - f(0)$ are drawn in Figure 4. It can be verified that when $\beta < \beta_2$ the only possible competitor for a minimizer prescribes $[u^*](x_1) = 0$, whereas when $\beta > \beta_2$, we need to consider the only case $[u^*](x_1) = KL\beta/(\rho_{\max}L + K - 1)$.

Case 1c. Finally, when $K > 1 + 2\rho_{\max}L$ we have $\alpha > \frac{2}{3}$ and consequently $\beta_2 < \beta_1$. Again, $f(p)$ is concave for $0 < p < \sqrt{1/3}$ and convex for $\sqrt{1/3} < p < \sqrt{\alpha\beta}$. Now for $0 < \beta < \beta_2$ we have $f(\sqrt{\alpha\beta}) > f(0)$ and $f'(\sqrt{\alpha\beta}) > 0$; when $\beta_2 < \beta < \beta_1$, $f(\sqrt{\alpha\beta}) < f(0)$ and $f'(\sqrt{\alpha\beta}) > 0$; when $\beta > \beta_1$, $f(\sqrt{\alpha\beta}) < f(0)$ and $f'(\sqrt{\alpha\beta}) < 0$. The analysis of the graphs of $f(p) - f(0)$, drawn in Figure 5, shows again the possibility of only one optimal value for p,

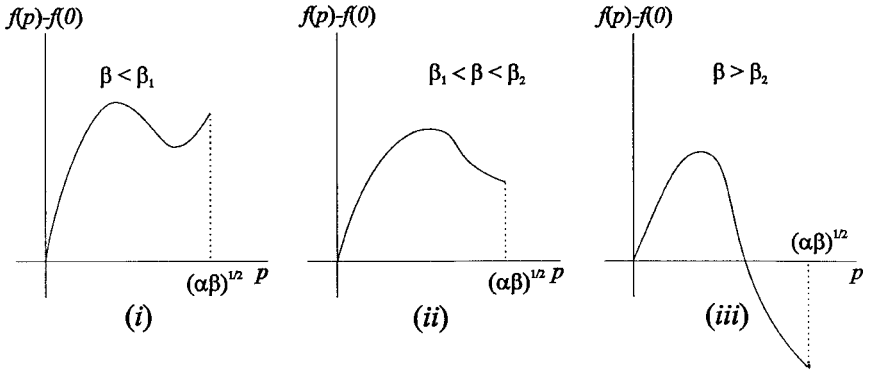

Figure 4. Graphs of $f(p) - f(0)$ for (i) $0 < \beta < \beta_1$, (ii) $\beta_1 < \beta < \beta_2$ and (iii) $\beta > \beta_2$. Case $1/3 < \alpha < 2/3$.

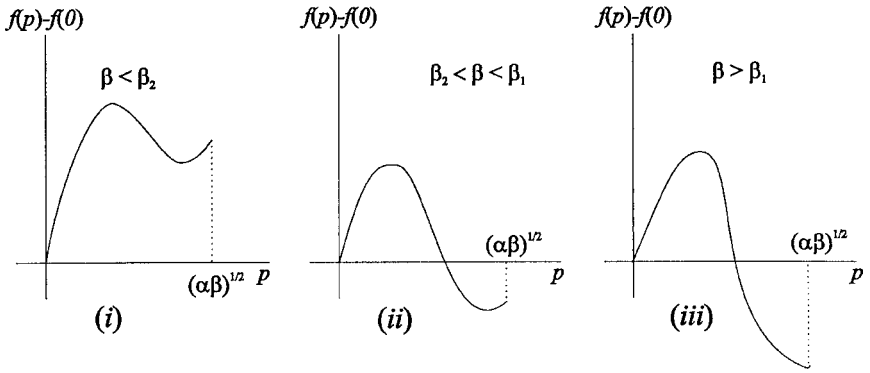

Figure 5. Graphs of $f(p) - f(0)$ for (i) $0 < \beta < \beta_2$, (ii) $\beta_2 < \beta < \beta_1$ and (iii) $\beta > \beta_1$. Case $\alpha > 2/3$.

say $p = \overline{p}$, such that $0 \leqslant \overline{p} \leqslant \sqrt{\alpha\beta}$. In particular, $\overline{p} = \sqrt{\alpha\beta}$, that is $[u^*](x_1) = KL\beta/(\rho_{\max}L + K - 1)$, for $\beta \geqslant \beta_1$.

Case 2. In the second case, for some positive constants e_0 and $[u^*]$, the function $e^*(x)$ takes the form

$$e^*(x) = \max\left\{e_0, [u^*]\frac{\rho(x - x_1)}{K}\right\}. \tag{A.14}$$

Since $\rho(\cdot)$ is smooth, even and unimodal, then $e^*(x) = e_0$ except for a neighborhood $|x - x_1| < \Delta$ of x_1, where

$$e^*(x) = [u^*]\frac{\rho(x - x_1)}{K} > 0, \qquad \mathrm{D}_a u^* = 0.$$

The quantity Δ is defined by the equation

$$e_0 = [u^*]\frac{\rho(\Delta)}{K}. \tag{A.15}$$

Consequently the integral condition becomes

$$\int_{|x-x_1|>\Delta}\left[e_0 - [u^*]\frac{\rho(x - x_1)}{K}\right]\mathrm{d}x = \beta L - [u^*].$$

By substituting e_0 from (A.15) we see that

$$[u^*] = \frac{K\beta L}{K - \int_{|x-x_1|>\Delta}\rho(x - x_1)\,\mathrm{d}x + \rho(\Delta)(L - 2\Delta)}, \tag{A.16}$$

and

$$e_0 = \frac{\beta L\rho(\Delta)}{K - \int_{|x-x_1|>\Delta}\rho(x - x_1)\,\mathrm{d}x + \rho(\Delta)(L - 2\Delta)}. \tag{A.17}$$

Noticing that

$$\frac{\mathrm{d}}{\mathrm{d}\Delta}\left[\rho(\Delta)(L - 2\Delta) - \int_{|x-x_1|>\Delta}\rho(x - x_1)\,\mathrm{d}x\right] = \rho'(\Delta)(L - 2\Delta)$$

we obtain from (A.16) and (A.17) that, since $\rho'(\Delta) < 0$ because $\rho(\cdot)$ is assumed unimodal,

$$\frac{\mathrm{d}[u^*]}{\mathrm{d}\Delta} = \frac{-K\beta L\rho'(\Delta)(L - 2\Delta)}{(K - \int_{|x-x_1|>\Delta}\rho(x - x_1)\,\mathrm{d}x + \rho(\Delta)(L - 2\Delta))^2} > 0 \tag{A.18}$$

and

$$\frac{\mathrm{d}e_0}{\mathrm{d}\Delta} = \frac{\beta L\rho'(\Delta)(K - \int_{|x-x_1|>\Delta}\rho(x - x_1)\,\mathrm{d}x)}{(K - \int_{|x-x_1|>\Delta}\rho(x - x_1)\,\mathrm{d}x + \rho(\Delta)(L - 2\Delta))^2} < 0 \tag{A.19}$$

so that

$$\frac{\mathrm{d}e_0}{\mathrm{d}\Delta} = -\frac{1}{K(L-2\Delta)}\left(K - \int_{|x-x_1|>\Delta} \rho(x-x_1)\,\mathrm{d}x\right)\frac{\mathrm{d}[u^*]}{\mathrm{d}\Delta}. \tag{A.20}$$

Now, recalling (A.14), define

$$\begin{aligned} g(\Delta) \;=\; & \int_{|x-x_1|>\Delta} U(e_0)\,\mathrm{d}x + \int_{|x-x_1|<\Delta} U\left([u^*]\frac{\rho(x-x_1)}{K}\right)\mathrm{d}x \\ & + \varphi\big([u^*](x_1)\big). \end{aligned} \tag{A.21}$$

We need to minimize this expression for $0 \leqslant \Delta \leqslant l_0$, being $|x - x_1| \leqslant l_0$ the support of the function $\rho(x-x_1)$. From (A.18) and (A.19), using for $U(\cdot)$ and $\varphi(\cdot)$ the expressions proposed in (6.1), recalling (A.15) and (A.20), we obtain

$$\begin{aligned} \frac{\mathrm{d}g(\Delta)}{\mathrm{d}\Delta} \;=\; & EA\frac{\rho(\Delta)}{K^2}[u^*]\frac{\mathrm{d}[u^*]}{\mathrm{d}\Delta}\left[\int_{|x-x_1|>\Delta} \rho(x-x_1)\,\mathrm{d}x - K\right. \\ & \left. + \frac{1}{\rho(\Delta)}\int_{|x-x_1|<\Delta} \rho^2(x-x_1)\,\mathrm{d}x + \frac{aK\sqrt{K(K-1)}}{[u^*]\rho(\Delta)L}\sqrt{\frac{L}{[u^*]}}\right]. \end{aligned} \tag{A.22}$$

For $\Delta \to l_0^-$ we have that $\rho(\Delta) \to 0$ and, from (A.17), that $[u^*] \to \beta L$. Besides, from (A.18) we have also

$$\frac{\mathrm{d}[u^*]}{\mathrm{d}\Delta} \to -\frac{1}{K}\beta L(L-2l_0)\rho'(l_0).$$

Consequently, we have from (A.22) that

$$\begin{aligned} & \lim_{\Delta\to l_0^-} \frac{\mathrm{d}g(\Delta)}{\mathrm{d}\Delta} \\ & = -\rho'(l_0)\frac{EA}{K^3}\beta^2L^2(L-2l_0)\left\{\int_{|x-x_1|<l_0} \rho^2(x-x_1)\,\mathrm{d}x + \frac{aK\sqrt{K(K-1)}}{L^2(\beta)^{3/2}}\right\}, \end{aligned} \tag{A.23}$$

and this quantity is non-negative since $\rho'(l_0) < 0$.

Considering the case $\Delta \to 0^+$, we find that $\rho(\Delta) \to \rho_{\max}$, $[u^*] \to K\beta L/(\rho_{\max}L + K - 1)$ and $\mathrm{d}[u^*]/\mathrm{d}\Delta \to -K\beta L\rho'(0^+)/(\rho_{\max}L + K - 1)^2$. Consequently, we now find

$$\begin{aligned} \lim_{\Delta\to 0^+} \frac{\mathrm{d}g(\Delta)}{\mathrm{d}\Delta} \;&=\; \lim_{\Delta\to 0^+} -\rho'(\Delta)\frac{EA\rho_{\max}\beta^2L^2}{(\rho_{\max}L + K - 1)^3}\left(1 - K + \frac{a(K-1)^2}{\rho_{\max}L^2(\alpha\beta)^{3/2}}\right) \\ &=\; 0, \end{aligned} \tag{A.24}$$

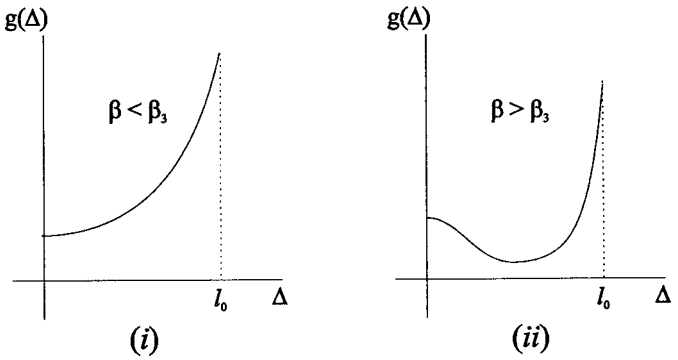

Figure 6. Graphs of $g(\Delta)$ for (i) $0 < \beta < \beta_3$, (ii) $\beta > \beta_3$.

where α has been defined in (A.7). Introducing

$$\beta_3 = \frac{1}{\alpha}\left(\frac{a(K-1)}{\rho_{\max}L^2}\right)^{2/3},$$

we distinguish two cases.

Case 2a. Let $\beta < \beta_3$. Then $\mathrm{d}g(\Delta)/\mathrm{d}\Delta > 0$ in a right neighborhood of $\Delta = 0$. Besides, noticing that

$$\begin{aligned}&\frac{\mathrm{d}}{\mathrm{d}\Delta}\left(\int_{|x-x_1|>\Delta}\rho(x-x_1)\,\mathrm{d}x + \frac{1}{\rho(\Delta)}\int_{|x-x_1|<\Delta}\rho^2(x-x_1)\,\mathrm{d}x\right)\\ &\quad = -\frac{\rho'(\Delta)}{\rho^2(\Delta)}\int_{|x-x_1|<\Delta}\rho^2(x-x_1)\,\mathrm{d}x \geqslant 0\end{aligned}$$

we obtain from (A.22) that $\mathrm{d}g(\Delta)/\mathrm{d}\Delta > 0$ for $0 < \Delta \leqslant l_0$. The graph of $g(\Delta)$ is qualitatively represented in Figure 6(i). It follows that when $\beta < \beta_3$ the only possible competitor is the value $\Delta = 0$. But since this configuration coincides with the limit value $[u^*](x_1) = (K\beta L)/(\rho_{\max}L + K - 1)$ in (A.3), we go back to the discussion of case 1.

Case 2b. Let us assume instead that $\beta > \beta_3$. Now $\mathrm{d}g(\Delta)/\mathrm{d}\Delta < 0$ in a right neighborhood of $\Delta = 0$, whereas

$$\left.\frac{\mathrm{d}g(\Delta)}{\mathrm{d}\Delta}\right|_{\Delta=l_0^-} > 0.$$

Thus, the graph of $g(\Delta)$ is now as in Figure 6(ii). It follows that there exists an optimal value of the jump comprised between $K\beta L/(\rho_{\max}L + K - 1)$ and βL.

In summary, for β sufficiently small, no jump occurs and consequently $u^*(x)$ is a linear function (i.e. $\mathrm{D}_a u^* = \beta$). For larger values of β, an optimal value of the jump can be calculated from an examination of the aforementioned cases.

References

1. L. Ambrosio, A compactness theorem for a special class of functions of bounded variation. *Boll. Un. Mat. Ital. B* **30** (1989) 857–881.
2. L. Ambrosio, N. Fusco and D. Pallara, *Functions of Bounded Variations and Free Discontinuity Problems*. Oxford Univ. Press, Oxford (2000).
3. G.I. Barenblatt, The mathematical theory of equilibrium cracks in brittle fracture. *Adv. in Appl. Mech.* **7** (1962) 44–129.
4. Z. Bažant and J. Planas, *Fracture and Size Effect in Concrete and Other Quasi-Brittle Materials*. CRC Press, New York (1998).
5. D. Broek, *The Practical Use of Fracture Mechanics.* Kluwer, Dordrecht (1989).
6. S. Cedolin, S. Dei Poli and I. Iori, Tensile behavior of concrete. *ASCE J. Engrg. Mech.* **113** (1987) 431–449.
7. E.A. Davis, The effect of the speed of stretching and the rate of loading on the yielding of mild steel. *ASME J. Appl. Mech.* (1938) A137–A140.
8. G. Del Piero, Towards an unified approach to fracture, yielding and damage. In: E. Inan and K.Z. Markov (eds), *Proc. of the 9th Internat. Symp. on Continuum Models and Discrete Systems.* World Scientific, Singapore (1998) pp. 679–692.
9. G. Del Piero, One-dimensional ductile-brittle transition, yielding and structured deformations. In: P. Argoul, M. Frèmond and Q.S. Nguyen (eds), *Variations de Domaines et Frontières Libres en Mécanique des Solides*. Kluwer, Dordrecht (1999).
10. G. Del Piero and L. Truskinovsky, Macro- and micro-cracking in one-dimensional elasticity. *Internat. J. Solids Struct.* **38** (2001) 1135–1148.
11. D.S. Dugdale, Yielding of steel sheets containing slits. *J. Mech. Phys. Solids* **8** (1960) 100–108.
12. C.F. Elam, *Distortion in Metal Crystals*. Claredon Press, Oxford (1935).
13. R. Fosdick and D. Mason, Single phase energy minimizers for materials with nonlocal spatial dependence. *Quart. Appl. Math.* **54** (1996) 161–195.
14. M. Froli and G. Royer-Carfagni, On discontinuous deformation of tensile steel bars: Experimental results. *ASCE J. Engrg. Mech*. **125** (1999) 1243–1250.
15. M. Froli and G. Royer-Carfagni, A mechanical model for elastic-plastic behavior of metallic bars. *Internat. J. Solids Struct.* **37** (2000) 3901–3918.
16. A. Hillerborg, M. Modèer and P.E. Petersson, Analysis of crack formation and crack growth in concrete by means of fracture mechanics and finite elements. *Cement Concrete Res.* **6** (1976) 773–782.
17. J. Planas, M. Elices and G.V. Guinea, The extended cohesive crack. In: G. Bakker and B.L. Karihaloo (eds), *Fracture of Brittle Disordered Materials: Concrete, Rock and Ceramics*. E. & FN Spon, London (1995) pp. 51–65.